

Dynamics of ferroelastic domains in ferroelectric thin films

V. NAGARAJAN¹, A. ROYTBURD¹, A. STANISHEVSKY¹, S. PRASERTCHOUNG¹, T. ZHAO¹, L. CHEN¹, J. MELNGAILIS¹, O. AUCIELLO² AND R. RAMESH^{*1}

¹Materials Research Science and Engineering Center, University of Maryland, College Park, Maryland 20742, USA

²Materials Science Division, Argonne National Laboratory, Argonne, Illinois 60439, USA

*e-mail: rramesh@eng.umd.edu

Published 22 December 2002; doi:10.1038/nmat800

Dynamics of domain interfaces in a broad range of functional thin-film materials is an area of great current interest. In ferroelectric thin films, a significantly enhanced piezoelectric response should be observed if non-180° domain walls were to switch under electric field excitation. However, in continuous thin films they are clamped by the substrate, and therefore their contribution to the piezoelectric response is limited. In this paper we show that when the ferroelectric layer is patterned into discrete islands using a focused ion beam, the clamping effect is significantly reduced, thereby facilitating the movement of ferroelastic walls. Piezo-response scanning force microscopy images of such islands in $\text{PbZr}_{0.2}\text{Ti}_{0.8}\text{O}_3$ thin films clearly point out that the 90° domain walls can move. Capacitors $1\ \mu\text{m}^2$ show a doubling of the remanent polarization at voltages higher than $\sim 15\ \text{V}$, associated with 90° domain switching, coupled with a d_{33} piezoelectric coefficient of $\sim 250\ \text{pm V}^{-1}$ at remanence, which is approximately three times the predicted value of $87\ \text{pm V}^{-1}$ for a single domain single crystal.

Ferroelectric materials such as lead zirconate titanate (PZT) offer a wide range of properties that make them very attractive candidates for a variety of microelectronic and sensing applications¹. For almost all these applications, domain-wall motion (both 180° and 90° domain walls, where the latter is elastic) in these materials has been identified as the key physical phenomenon, and hence a subject of intense scientific research. In bulk ceramic or single crystals of prototypical perovskites (such as PZT and barium titanate), piezoelectric phenomena arising from 90° domain-wall contributions were extensively studied in the 1950s and 1960s^{2,3}. More recently, 90° domain movement has been observed by transmission electron microscopy in single crystal BaTiO_3 and KaNbO_3 (V. P. Dravid, unpublished results and ref. 4). The reason to particularly study the piezoelectric contribution of 90° domain walls stems from the fact that when these domain walls move, they can greatly enhance the piezoelectric coefficient.

The motivation to engineer such extrinsic contributions from 90° domain walls in thin films comes from potential silicon-based microelectromechanical system (MEMS) sensor and actuator applications. However, in thin films the piezo response is determined by the elastic interaction between the film and the substrate; the clamping imposed by the substrate greatly curbs the movement of such ferroelastic domains^{5,6} as well as the intrinsic piezoelectric response. The role of domain pinning as a factor limiting the contribution of 90° domain walls to the overall piezoelectric response has been suggested^{7,8}, and although the conclusion from X-ray diffraction was that the movement of 90° domain walls in thin epitaxial films is possible, there was no report of any enhancement of the piezo response compared with theoretically predicted values for a single crystal. The contribution of 90° wall movement to the piezoelectric coefficient, d_{33} , in a clamped film has been calculated⁹ to be $\sim 40\text{--}70\ \text{pm V}^{-1}$. However, displacement of 90° domain walls in an unclamped film should lead to strains of the order of the lattice tetragonality¹⁰, and therefore a d_{33} significantly larger than that predicted for single domain crystals. Thus, to relieve the effect of clamping, it is necessary to create structures with lateral dimensions of the same order as the thickness of the film¹¹. A fourfold enhancement in piezoelectric response in dry etched islands (smaller than 300 nm in

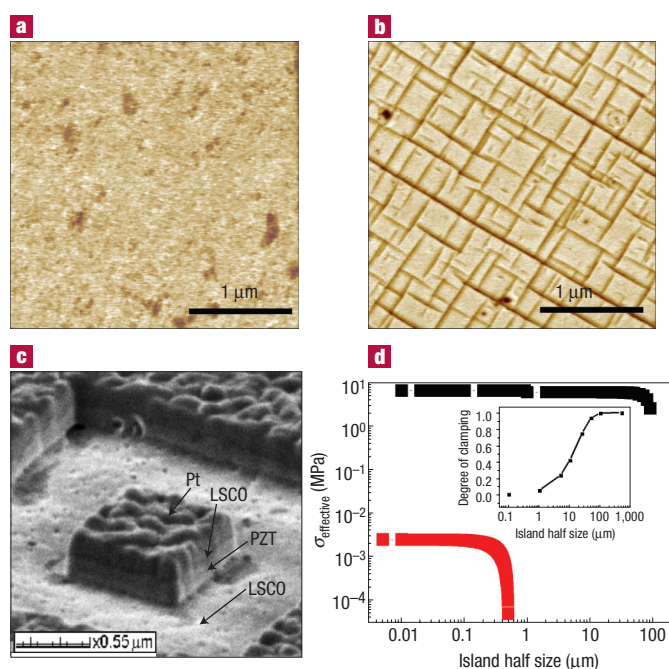


Figure 1 PZT film architectures and nanostructuring effects. **a, b**, Piezo-SFM images of epitaxial films 100 nm (**a**) and 300 nm (**b**) thick. The 300 nm film clearly shows a periodic 90° domain structure, which is absent in the 100 nm film. **c**, SEM image of a $1 \mu\text{m}^2$ island with the top electrode. **d**, Effective stress distribution for the $1 \mu\text{m}$ (red) and $200 \mu\text{m}$ (black) capacitors. The inset shows the degree of clamping plotted as a function of the lateral capacitor size for $1 \mu\text{m}$ thick film.

lateral size) of $\text{PbZr}_{0.4}\text{Ti}_{0.6}\text{O}_3$ thin films has been claimed¹². This increase was attributed to the removal of 90° domain walls during the thermal annealing after dry etching; however, because the piezo response was presented in arbitrary units, it is difficult to compare it to theoretically predicted values. In contrast, our research is aimed at the tantalizing

possibility of movement of such domain walls in thin films under an applied electric field. Through direct observations and quantitative measurements, we clearly show that ferroelectric islands still have a large fraction of 90° domains, and that these domains move on application of an electric field, thereby enhancing the d_{33} above and beyond that predicted for a single domain single crystal.

Epitaxial PZT (0/20/80) thin films of varying thickness (from 100 nm to $1 \mu\text{m}$) were deposited onto single crystal (100) SrTiO_3 substrates by pulsed laser deposition. To facilitate heteroepitaxy, we used conducting perovskite LSCO (La-Sr-Co-O_3) as bottom and top electrodes, also deposited by pulsed laser deposition. Details of the deposition process are described in an earlier paper¹³. Scans of θ - 2θ using a four-circle X-ray diffractometer (D500, Bruker-AXS, Madison, Wisconsin, USA) revealed a mixture of c -axis domains (with polarization normal to the film) and 90° domains (with polarization in the plane of the film) with the absence of any secondary phases. The 90° -domain volume fraction was calculated from the ω -rocking curves. To eliminate substrate-induced clamping, $1 \mu\text{m}^2$ and smaller capacitors or islands were fabricated using Ga^+ focused ion-beam (FIB) milling¹⁴. An accelerating voltage of 50 kV, dose of 8×10^{17} ions cm^{-2} and a beam size of 6–20 nm (MICRION2500, Hillsboro, Oregon, USA) was used to delineate the structures. The domain structure for such islands (without a top electrode) was imaged by Piezo-response scanning force

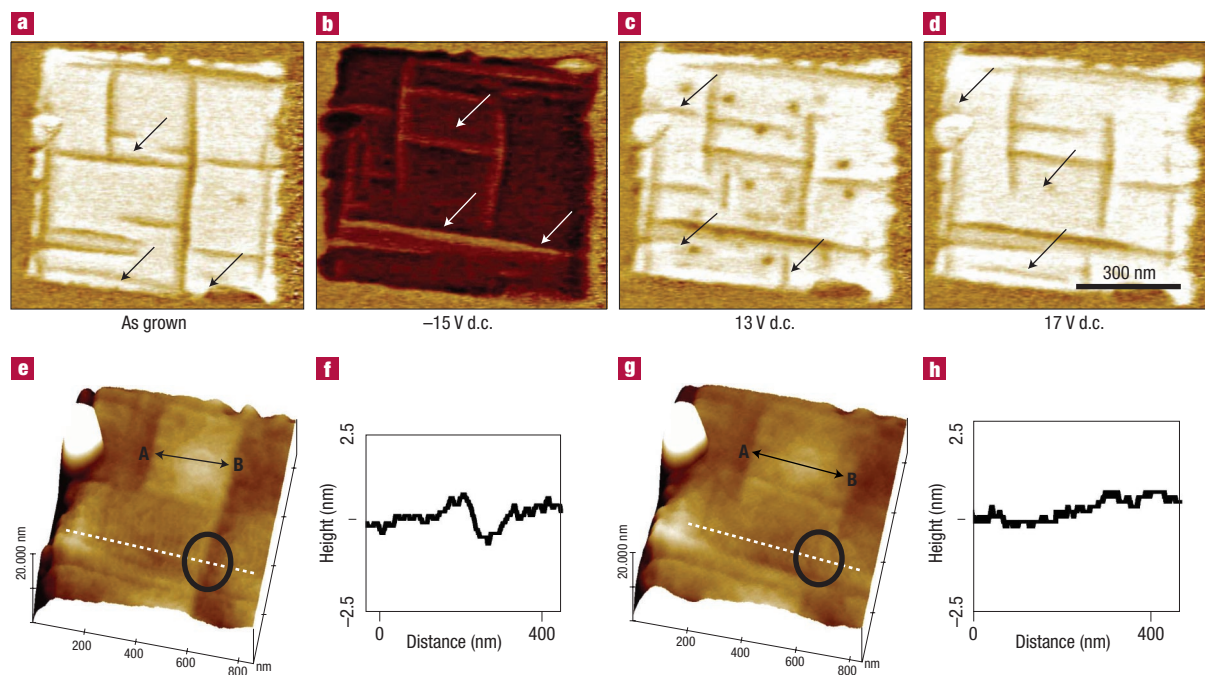


Figure 2 The evolution of the ferroelastic domain structure as a function of applied electric field for a $1 \mu\text{m}^2$ island. **a–d**, Piezo response images of a $1 \mu\text{m}^2$ island after application of various d.c. bias voltages. The scale for **a–c** is as for **d, e**. The topography of the surface before and **g**, after the application of the electric field. **f**, The AFM line trace across the region identified by the circle in **e** clearly shows a surface height change of $\sim 20 \text{ \AA}$, which corresponds to the difference in surface displacement between the c - and a -domains. **h**, The AFM profile for the same region (and circled in **g**) shows no such discontinuity indicating that the 90° domain has moved.

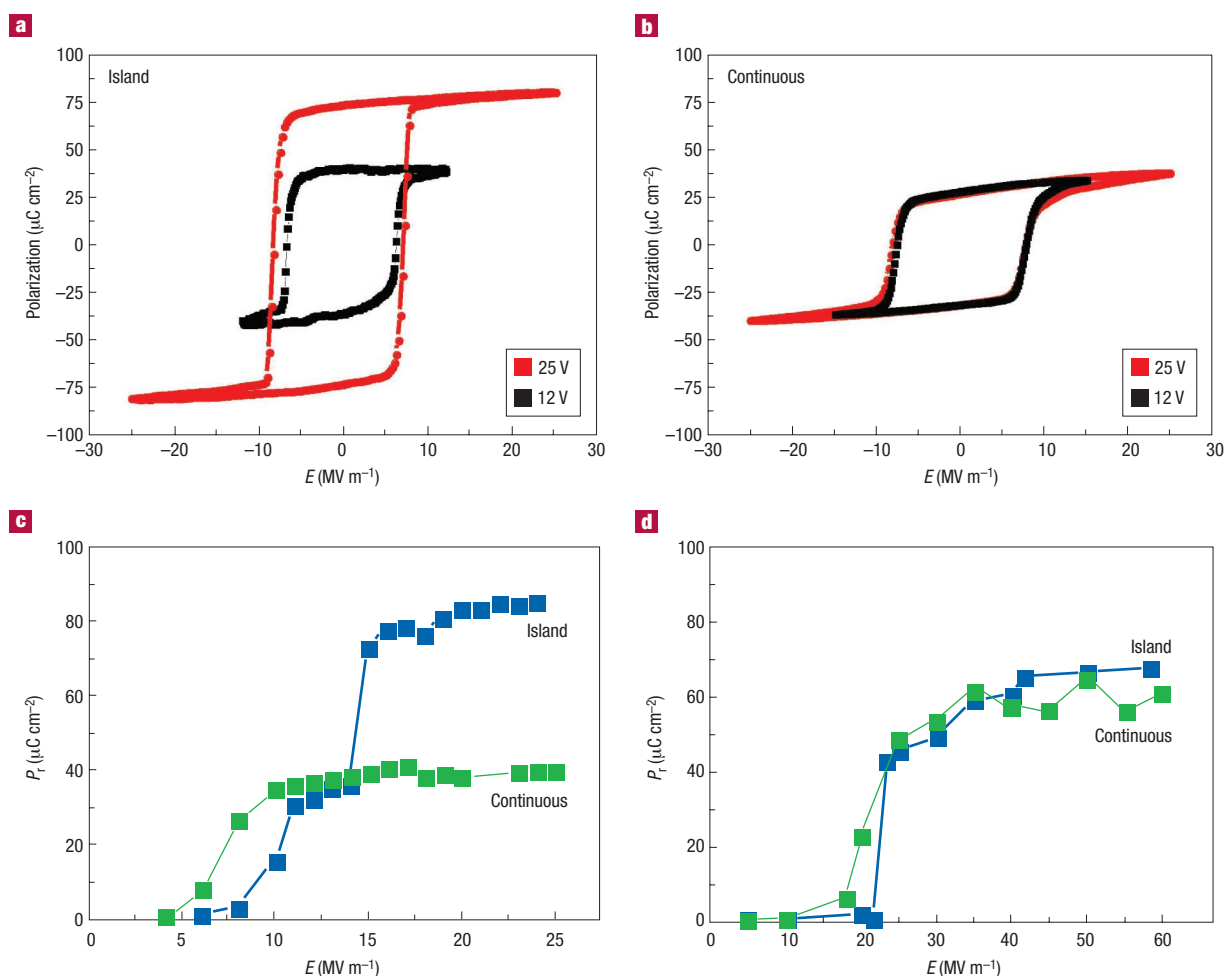


Figure 3 The effect of the movement of ferroelastic domains on the polarization response of a nanostructured island compared to a continuous film. Ferroelectric polarization loops for **a**, the 1 μm^2 island and **b**, the continuous film. **c**, A comparison of the voltage dependence of remanent polarization (P_r), for the 1 μm^2 island and the continuous film. **d**, Voltage dependence of P_r for island and continuous capacitor on the 100-nm-thick film. E is the applied electric field.

microscopy (Piezo-SFM, Digital Instruments, Santa Barbara, California, USA). Piezo-SFM is based on the detection of the local electromechanical vibration of the ferroelectric sample caused by an external a.c. voltage¹⁵. The voltage is applied through the probing tip, which is used as a movable top electrode. Finally, for quantitative d_{33} measurements, a LSCO/PZT/LSCO heterostructure was used with a platinum layer deposited over the top LSCO electrode. To calibrate the output signal from the photodiode we used x-cut quartz coated with top and bottom Au electrodes. The quartz was driven from 0 to 10 V and the displacement of the tip was recorded. The slope of the linear displacement versus voltage plot is equal to d_{33} of quartz, that is, 2.3 pm V⁻¹.

Figure 1a,b shows piezo response images of films 100 nm and 300 nm thick. Consistent with previous work, the 100 nm film (Fig. 1a) has no discernible 90° domains^{13,16}; films thicker than 150 nm relax the transformation strain through the formation of a two-dimensional array of 90° domains (see Fig. 1b). In the as-grown condition, the 90° domains appear as orthogonal needle-shaped features in a matrix that is c-axis oriented. Quantitative X-ray diffraction measurement yields a 90° domain fraction of ~30% for the 300 nm film, increasing to ~50% at a thickness of 1 μm . Figure 1c shows a scanning electron micrograph (SEM, Micrion2500) image of a 1 μm^2 island with the top electrode that

was used for the quantitative piezoelectric measurements. The decrease in piezodeformation due to clamping is directly related to the compliance of the PZT film and the substrate. As follows from Lefki and Dormans⁶ the measured converse d_{33} of a thin-film capacitor can be correlated to the intrinsic d_{33} of the unclamped single domain, single crystal through the equation:

$$d_{33}^{\text{measured}} = d_{33} - \frac{2s_{13}^E \sigma_{\text{effective}}}{E_3} \quad (1)$$

where the first term on the right hand side is the intrinsic d_{33} and the second term is due to the constraint imposed by the substrate. $\sigma_{\text{effective}}$ is an effective stress in the film due to the inability of the surface to deform fully in response to the electric field, and is a measure of the degree of clamping. E is the electric field applied to measure the piezo response, and s_{13}^E is the compliance. Continuum mechanics approaches, based on the continuity of displacements across the film–substrate interface^{17,18} allow one to calculate this effective stress (degree of clamping) as a function of the lateral island size for a fixed film thickness. From an approximate analysis¹⁸ the effective stress can be estimated from the equation:

$$\sigma_{\text{effective}} = Y_f^0 \chi_0 \epsilon_{\text{effective}} \quad (2)$$

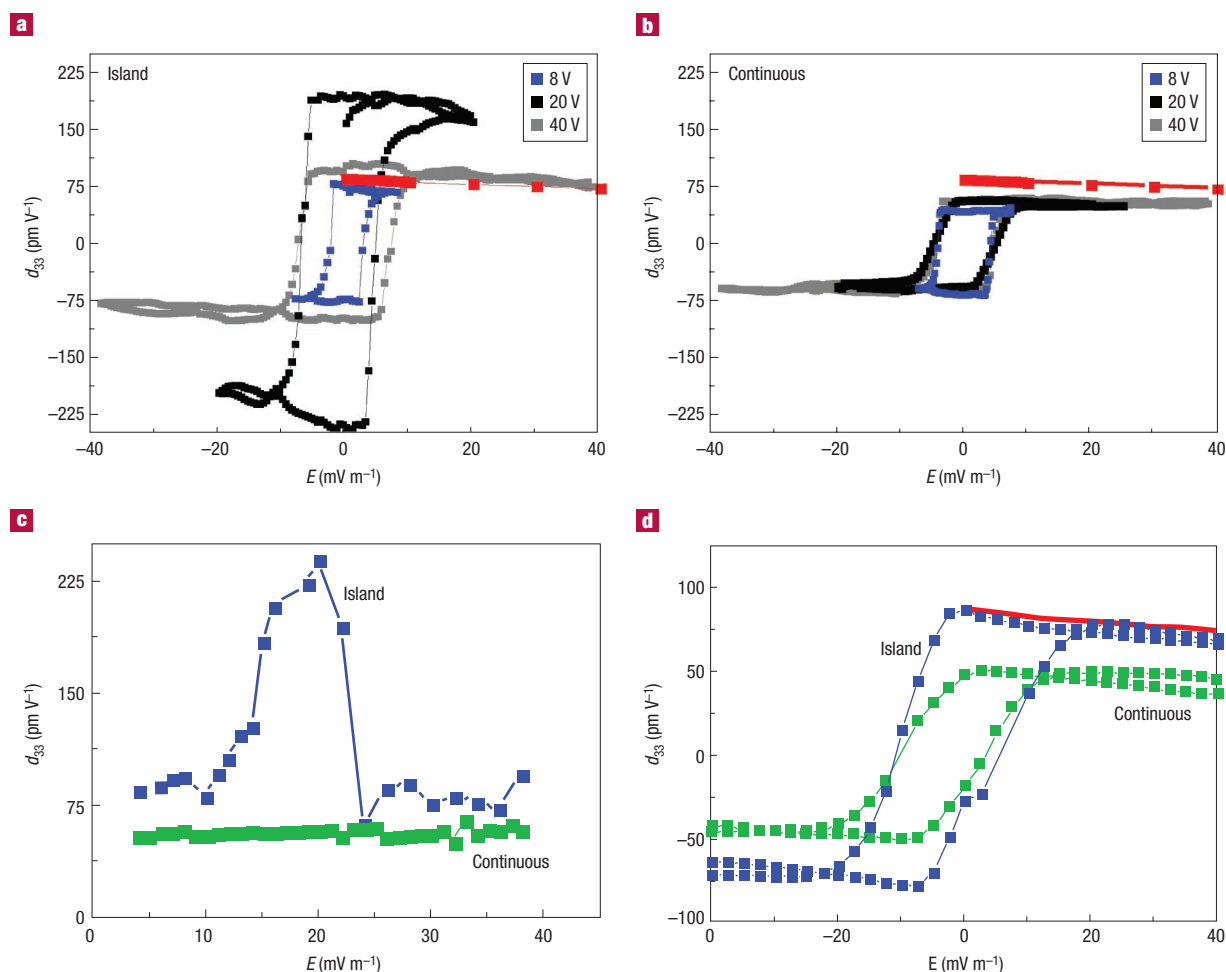


Figure 4 Piezoelectric measurements of the island compared with the continuous capacitors. Piezoelectric loops for **a**, the 1 μm² island and **b**, the continuous film as function of different applied field, E . **c**, A comparison of the voltage dependence of d_{33} for the 1 μm² island and the continuous film. **d**, Piezoelectric loops for the island and continuous film. The red line in **a**, **b**, and **d** is the theoretically predicted single crystal, single domain curve.

where $\chi_0(x) = 1 - e^{-k(l-x)}$ is the distribution function of the stress as a function of the island half length, l , x is the spatial variable, k is the effective modulus, and Y_f^0 is the generalized Young's modulus of the film $Y_f^0 = Y/(1 - \nu)$, where ν is Poisson's ratio. $\epsilon_{\text{effective}}$ is the in-plane strain corresponding to the clamping stress, $\sigma_{\text{effective}}$, and is obtained from $\epsilon_{\text{effective}} = d_{31} \times E$ where E is the electric field applied to measure the piezo response.

The effect of FIB milling on the degree of clamping calculated using equation (2) is shown in Fig. 1d, which is a simulation of the distribution of $\sigma_{\text{effective}}$ along (x) for a 1 μm² island and a continuous capacitor (~200 μm) in a film 1 μm thick. Compared with the continuous capacitor, the magnitude of $\sigma_{\text{effective}}$ at the centre ($x = 0$) drops by approximately three orders of magnitude in the island. At the edge of the capacitor, $\sigma_{\text{effective}}$ drops sharply towards zero, indicating that the edges are fully unclamped. The inset shows that the degree of clamping drops to almost zero when the lateral dimension is ~1 μm or smaller and for sizes greater than 10 μm, it rapidly climbs towards a fully clamped state. Our finite element analyses are also consistent with the conclusions described in Fig. 1d.

Figure 2a–d show piezo response images of a 1 μm² island at various d.c. bias voltages. In the as-grown condition (Fig. 2a) the 90° domains appear as needle-shaped features in a matrix that is c -axis oriented. On the

application of a d.c. bias the image contrast reverses. For example, at –15 V (Fig. 2b) the overall image contrast has reversed (from bright to dark) as a consequence of 180° domain switching in the matrix. However, accompanying this 180° domain reversal is a significant displacement of the 90° domains, as indicated by arrows in Fig. 2a,b. Such displacements of the 90° domains continue on reversal of the d.c. bias, as illustrated in Fig. 2c,d and are confirmed through AFM traces of the film surface. Figure 2e, g shows the topography of the surface before and after the application of the electric field respectively. AFM line traces across the region identified by the circle in Fig. 2e show a measurable surface height change of ~20 Å. In earlier studies¹³ we have shown that this corresponds to the height change between c and a domains. This change in height is given as $\Delta z = t_d \times \tan^{-1}[(c/a) - 1]$ where t_d is the domain thickness (~50 nm) and c/a is the tetragonality of the film. When the 90° domain is eliminated from this location (Fig. 2g) the AFM profile shows no such discontinuity (Fig. 2h). We also see that the distance between points AB has increased from 220 nm in Fig. 2e to 350 nm in Fig. 2g, indicating a 90° domain displacement of approximately 130 nm. We note that 180° domain reversal is observed in all films, with or without a 90° domain structure.

Significant displacement of 90° domains during the application of the electric field should be accompanied by commensurate changes in

the remanent polarization, P_r , as well as in the piezo response, d_{33} . Piezo response force microscopy was used to quantitatively measure these properties for both the continuous films as well as the FIB-milled islands. Recognizing that the polarization and piezoelectric responses of these capacitors are a function of the electric field history, we carried out each set of experiments on fresh capacitors. Figure 3a,b shows ferroelectric polarization loops for the $1\ \mu\text{m}^2$ island and the continuous film, respectively. For clarity, we present hysteresis loops at two selected values of applied field, namely at 12 V and at 25 V (corresponding to fields of $12\ \text{MV m}^{-1}$ and $25\ \text{MV m}^{-1}$). In the case of the island (Fig. 3a) a dramatic increase in P_r is observed from $\sim 40\ \mu\text{C cm}^{-2}$ at 12 V to $\sim 80\ \mu\text{C cm}^{-2}$ at 25 V. In contrast, the continuous film in Fig. 3b shows no such increase, strongly suggesting that there is no significant change of the 90° domain fraction in such a fully clamped film. The study of P_r as a function of maximum applied field (Fig. 3c) clearly reveals a step-like change in the P_r for the island around 15 V, strongly suggesting the movement of 90° domains at this applied field. The P_r at high fields in this case is very close to that predicted theoretically¹⁹ for PZT (0/20/80); the doubling of P_r for the island compared with the continuous film is also consistent with the removal of a significant fraction of the 90° domains. Figure 3d compares the field-dependent switched polarization for an island and a continuous capacitor in a 100-nm-thick film. They show almost identical behaviour with each other, that is, a P_r of $\sim 70\ \mu\text{C cm}^{-2}$ is reached by both films, consistent with the fact that the 100-nm-thick film has no 90° domains.

These changes in P_r values should also be reflected in the voltage-dependent changes in d_{33} . Figure 4a,b shows the corresponding d_{33} loops measured for the $1\ \mu\text{m}^2$ island and the continuous film, respectively. Theoretically calculated values of d_{33} versus applied field, obtained using a Ginzburg–Landau–Devonshire formalism for a single domain $\text{PbZr}_{0.2}\text{Ti}_{0.8}\text{O}_3$ bulk crystal¹⁹ are also plotted in this figure; the theoretical value of d_{33} in a single domain single crystal at remanence is $87\ \text{pm V}^{-1}$. We consider the experimental results for the $1\ \mu\text{m}^2$ island first. At an applied voltage of 8 V the piezo loop shows a remanent d_{33} of $\sim 100\ \text{pm V}^{-1}$. At 20 V we were able to obtain a piezo loop with a remanent d_{33} value of $\sim 250\ \text{pm V}^{-1}$, which is about three times larger than that predicted theoretically and five times the clamped value. Finally, at 40 V, the piezo loop has dramatically shrunk and the d_{33} value at remanence is $\sim 90\ \text{pm V}^{-1}$. We note that this value is, within experimental error, close to that predicted by theory for a single domain single crystal, suggesting that all mobile 90° domains have been removed from the island. As with the polarization data in Fig. 3b, we do not observe any significant changes in the piezo response of the continuous film (Fig. 4b), suggesting very little contribution from the displacement of 90° domains. Corresponding to the step in the polarization plot (Fig. 3c) there is a peak in the plot of d_{33} versus applied voltage (Fig. 4c) although the absolute maximum value of d_{33} is much lower than what would be expected. Finally, Fig. 4d compares the d_{33} for an island with a continuous film of film thickness 100 nm (Fig. 1a). The increase in d_{33} from $50\ \text{pm V}^{-1}$ (for the continuous capacitor) to $90\ \text{pm V}^{-1}$ is a consequence of elimination of clamping, equal to a piezo response that is predicted theoretically for a single domain single crystal (plot in red).

In summary, we present conclusive evidence for significant contributions from ferroelastic 90° domain movement to the ferroelectric and piezoelectric responses of epitaxial PZT films when the clamping imposed by the substrate is reduced. Delineating islands distinctly alters the substrate-imposed clamping thus facilitating domain movement. Finally, we note that this phenomenon should also be viable for a wide range of thin-film materials involving ferroelastic domains, such as ferromagnetic shape-memory alloys and martensites.

Received 22 August 2002; accepted 25 November 2002; published 22 December 2002.

References

- Auciello, O., Scott, J. F. & Ramesh, R. The physics of ferroelectric memories. *Phys. Today* **51**, 22–27 (1998).
- Little, E. Dynamic behavior of domain walls in Barium titanate. *Phys. Rev.* **98**, 978–984 (1955).
- Berlincourt, D. & Kreuger, H. H. A. Domain processes in lead titanate and barium titanate ceramics. *J. Appl. Phys.* **30**, 1804–1810 (1959).
- Krishnan, A., Treacy, M. M. J., Bisher, M. E., Chandra, P. & Littlewood, P. B. in *Fundamental Physics of Ferroelectrics 2000* (ed. Cohen, R. E.) 191–200 (American Institute of Physics, College Park, Maryland, USA, 2000).
- Lefki, K. & Dormans, G. J. M. Measurement of piezoelectric coefficients of ferroelectric thin films. *J. Appl. Phys.* **76**, 1764–1767 (1994).
- Tuttle, B. et al. *Relationships Between Ferroelectric 90 Degrees Domain Formation And Electrical Properties Of Chemically Prepared Pb(Zr,Ti)O₃ Thin films* (eds Auciello, O. & Waser, R.) (Kluwer, Dordrecht, 1995).
- Kohli, M., Murali, P. & Setter, N. Removal of 90° domain pinning in (100) $\text{Pb}(\text{Zr}_{0.15}\text{Ti}_{0.85})\text{O}_3$ thin films by pulsed operation. *Appl. Phys. Lett.* **72**, 3217–3219 (1998).
- Lee, K. S., Kim, Y. K., Baik, S., Kim, J. & Jung, I. S. *In situ* observation of ferroelectric 90° -domain switching in epitaxial $\text{Pb}(\text{Zr,Ti})\text{O}_3$ thin films by synchrotron x-ray diffraction. *Appl. Phys. Lett.* **79**, 2444–2446 (2001).
- Pertsev, N. A. & Emelyanov, A. Y. Domain wall contribution to the piezoelectric response of epitaxial ferroelectric thin films. *Appl. Phys. Lett.* **71**, 3646–3648 (1997).
- Burcsu, E., Ravindran, G. & Bhattacharya, K. Large strain electrostrictive actuation barium titanate. *Appl. Phys. Lett.* **77**, 1698–1700 (2000).
- Roytburd, A. L. et al. Measurement of internal stresses via the polarization in epitaxial ferroelectric films. *Phys. Rev. Lett.* **85**, 190–193 (2000).
- Buhlman, S., Dwir, B., Baborowski, J. & Murali, P. Size effect in mesoscopic epitaxial ferroelectric structures: Increase of piezoresponse with decreasing feature size. *Appl. Phys. Lett.* **75**, 3195–3197 (2002).
- Nagarajan, V. et al. Thickness dependence of structural and electrical properties in epitaxial lead zirconate titanate films. *J. Appl. Phys.* **86**, 595 (1999).
- Melngailis, J. Critical Review: Focused ion beam technology and applications. *J. Vac. Sci. Technol.* **B 5**, 469–495 (1987).
- Gruverman, A., Auciello, O. & Tokumoto, H. Imaging and control of domain structure in ferroelectric thin films via scanning force microscopy. *Ann. Rev. Mater. Sci.* **28**, 101–123 (1998).
- Kwak, B. S. et al. Strain relaxation by domain formation in epitaxial ferroelectric thin films. *Phys. Rev. Lett.* **68**, 3733–3736 (1992).
- Suhir, E. An approximate analysis of stresses in multilayered elastic thin films. *J. Appl. Mech.* **55**, 143–148 (1998).
- Sauter, A. I. & Nix, W. D. Thermal stresses in aluminum lines bonded to substrates. *IEEE Trans. Compon. Hybr.* **15**, 594–600 (1992).
- Haun, M. J., Furman, E., Jang, S. J. & Cross, L. E. Thermodynamic theory of the lead zirconate-titanate solid solution system. *Ferroelectrics* **99**, 63–86 (1989).

Acknowledgements

This work was supported by a NSF-MRSEC Grant DMR 00-80008, NSF Grant DMR 0210512 and partly by a Department Of Energy S&P Center. We also acknowledge C. S. Ganpule for his contribution to the domain imaging studies and the effective stress calculations. Correspondence and requests for materials should be addressed to R.R.

Competing financial interests

The authors declare that they have no competing financial interests.